Optical Engineering

Formation mechanism of self-organized nanogratings on a titanium surface using femtosecond laser pulses

Md. Shamim Ahsan
Man Seop Lee

SPIE

Formation mechanism of self-organized nanogratings on a titanium surface using femtosecond laser pulses

Md. Shamim Ahsan
Korea Advanced Institute of Science and
    Technology
Photonics Application Lab
291 Daehak-ro (373-1 Guseong-dong)
Yuseong-gu, Daejeon 305-701, Republic of Korea
    and
Khulna University
Electronics and Communication Engineering
    Discipline
School of Science, Engineering, and Technology
Khulna 9208, Bangladesh
E-mail: shamim@kaist.ac.kr

Man Seop Lee
Korea Advanced Institute of Science and
    Technology
Photonics Application Lab
291 Daehak-ro (373-1 Guseong-dong)
Yuseong-gu, Daejeon 305-701, Republic of Korea
E-mail: leems1502@kaist.ac.kr

Abstract. We demonstrate the formation of self-organized nanogratings on a titanium surface under the irradiation of a single-beam femtosecond laser. Self-formed, periodic nanogratings are printed on a titanium surface by varying the average pulse energy, pulse width, and number of laser pulses in each spot. The direction of the nanogratings is perpendicular to the direction of the laser polarization. The nanograting period shows obvious dependence on the average pulse energy, pulse width, and number of laser pulses. The period of the self-organized nanogratings shows an increasing trend with the increase of laser energy and pulse width, and a decreasing trend with an increase of number of applied laser pulses. We qualitatively explain the formation mechanism of the self-organized nanogratings and their dependence on various laser parameters. © 2012 Society of Photo-Optical Instrumentation Engineers (SPIE). [DOI: 10.1117/1.OE.51.12.121815]

1 Introduction

Since the discovery of the functional coherent laser radiation in 1960, lasers have been considered as a promising tool for material processing such as ablation, cutting, drilling, marking, cleaning, welding, and forming a variety of structures in different materials.[1] During the last few decades, the demand for new laser sources with higher precision, higher resolution, and better surface and volume localization has increased due to the expansion of the application areas of laser engineering, such as optoelectronics, microelectronics, nanoscience and nanotechnology, and biology. As a result, various new laser sources, including ultrafast laser sources (e.g., picosecond, femtosecond, and attosecond laser), ultraviolet laser sources (e.g., excimer laser and harmonics of solid state laser), and low-cost laser sources (e.g., diode laser and fiber laser), become available.[2] The advent of femtosecond lasers has opened a new era for micro- and nano-machining of various materials.[3–8]

In recent years, the formation of laser-induced periodic surface structure (LIPSS) and nanostructure-covered LIPSS (NC-LIPSS), based on femtosecond lasers, has been reported in detail by many researchers on different materials: glasses,[9–11] indium tin oxide (ITO),[12] indium phosphide (InP),[13] and metals.[14–21] The formation mechanism of LIPSS, formed on a material surface, has been described from different physical perspectives. Bonse et al.[13] have presented a comprehensive study on the formation of LIPSS in InP, indicating the influence of the number of irradiated laser pulses on the period of LIPSS. Periodic modulation of the absorbed light intensity, due to the interference between the incident linearly polarized laser beam and the surface wave (generated by scattering during the pulse

duration) is considered as the formation mechanism of the LIPSS. The dependence of the LIPSS period printed on a platinum surface on the number of irradiated laser pulses is reported by Vorobyev et al.,[14] where the interference of the incident laser beam and the excited localized and propagating surface plasmons (which increases with the increasing number of laser pulses) is considered as the mechanism of LIPSS formation. Huang et al.[15] reported the orientation and the period of high-spatial-frequency LIPSS (HSFL), parallel to the electric field, and low-spatial-frequency LIPSS (LSFL), perpendicular to the electric field, on a titanium surface, where the result is interpreted by the theoretical model of Bonch-Bruevich et al.[22] In Ref. 16, Qi et al. investigated the evolution of HSFL (at the edge of the irradiated spot) and LSFL (at the central part of the ablated area) on a stainless steel surface and their dependence on laser fluence and the number of laser pulses, where both the HSFL and LSFL are perpendicular to an electric field vector. A parametric decay model (stimulated Raman scattering) has been proposed[17,18] to explain the mechanism for self-formed LIPSS on a variety of metal surfaces and their dependence on laser fluence. Golosov et al.[19] have reported the formation of LIPSS on a titanium surface, where the grating period depends on the wavelength of the incident light, the incident angle of the laser beam, and the laser fluence. Effects of electron-phonon coupling and electron diffusion on LIPSS growth have been studied by Colombier et al.[20] One of the most remarkable models is reported by Golosov et al.,[21] where one-dimensional (1-D) nanogratings with subwavelength spacing are considered as the harmonics of surface nano-relief. According to the authors, the nano-relief is formed due to the diffraction of the incident laser beam from an intermediate nonharmonic periodic surface grating, which is evolved during the initial laser pulses due to the interference by a

surface electromagnetic wave (SEW) excited by them and its subsequent ablation resulting from the interference maxima. However, none of the aforementioned papers report the dependence of a nanograting's period on the pulse width of femtosecond laser pulses.

In this paper, we describe a study of the evolution of self-organized nanogratings (i.e., LIPSS) on a titanium surface using near-infrared femtosecond laser pulses, including a comprehensive analysis of the influence of laser parameters: the average pulse energy, pulse width, and number of laser pulses in each irradiated spot. This paper principally deals with the HSFL, which is evolved in the peripheral area of the irradiated spots. From the experimental results, it is obvious that the self-formed nanogratings are printed perpendicular to the laser polarization direction. The key discovery of our investigation is the dependence of a nanograting's period on various laser parameters, especially on the pulse width. We strongly believe that our experimental results can provide an in-depth understanding of the interactions of femtosecond laser pulses with a titanium surface.

2 Experimental Details

In order to carry out our experiments, we used a Ti:sapphire femtosecond laser (IFRIT-LH-C031; Cyber Laser Inc., Tokyo, Japan) operating at the central wavelength of 786 nm. The pulse repetition rate (R_p) of the laser system was fixed at 1 kHz. The femtosecond laser beam was focused onto the titanium surface at normal incidence through a 50× achromatic objective lens (M Plan Apo NIR; Mitutoyo, Kawasaki, Japan) with focal length of 17 mm and numerical aperture (NA) of 0.42. The experimental setup for the

formation of the nanogratings on the titanium sample is represented in Fig. 1(a) and 1(b).

The laser beam was guided toward the sample surface by mirrors. An external mechanical shutter was utilized to control the exposure time. We used a computer-controlled linear translation stage (laser physics) with a resolution of 100 nm to position the laser beam in the x, y, and z directions. A continuously variable attenuator/beam-splitter (Newport) was utilized to adjust the power/energy of laser pulses. A rotating quartz phase $\lambda/2$ wave plate was placed in the incident polarized laser beam. The polarizing cube beam-splitter reflects s-polarized light in the perpendicular direction while transmitting p-polarized light. The amount of power attenuation depends on the degree of rotation of the attenuator. A titanium sample with a thickness of 100 μm, mean roughness (Ra) of 32 nm, and a complex refractive index of $\tilde{\eta} = \eta + ik = 4.33 + i5.29$ at 786 nm was used in the experiment. A power meter (FM/GS; Coherent, Santa Clara, CA) was used to measure the average power of the laser pulses after the objective lens.

Atomic force microscope (AFM) (D3100; Bruker, California, USA) was used to investigate the surface roughness of the titanium sample. A three-dimensional (3-D) AFM image of the sample surface prior to laser application is depicted in Fig. 1(c). We used the single-beam direct laser writing (SBDLW) technique[23] to fabricate self-organized nanogratings on the titanium surface. Before laser micromachining, the sample was cleaned by 99% ethyl alcohol. We varied laser parameters, including the average pulse energy, pulse width, and number of laser pulses for each irradiated spot. The average pulse energy (E_L) of the femtosecond laser pulses was in the range of 93 to 248 nJ. The pulse
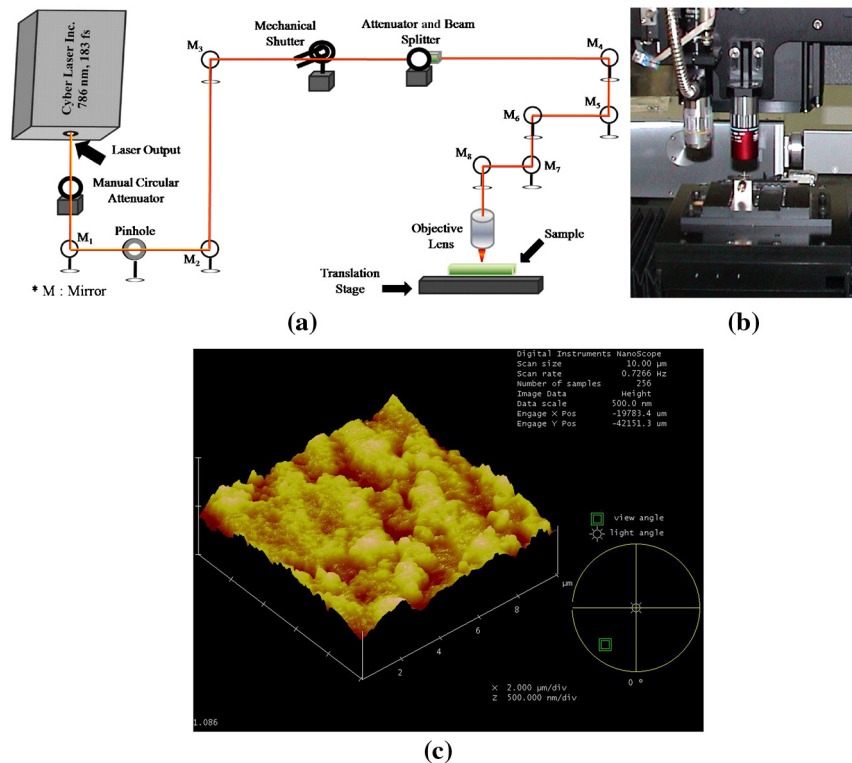

Fig. 1 Experimental details. (a) Schematic diagram of the experimental setup for writing self-formed nanogratings on the titanium surface. (b) Photograph of the experimental setup of (a). (c) 3-D AFM image of the titanium sample surface.

width (τ) used during the experiment was either 183 or 500 fs. The number of laser pulses in each spot (N) varied from 10 to 2000. Due to the application of a large number of laser pulses, self-organized nanogratings with variable period were printed on the titanium surface depending on the laser parameters. In order to analyze the surface morphology of the titanium sample, we used field-emission scanning electron microscope (FE-SEM) (S-4800; Hitachi, Tokyo, Japan) images of the sample surface.

3 Results

To examine the evolution of morphological changes due to the application of femtosecond laser pulses, a large number of identical pulses (varying from 10 to 2000) with variable laser parameters (laser energy: 93 to 248 nJ; pulse width:

183 fs or 500 fs) were applied on each irradiated spot of the titanium surface. As a result, LIPSSs of variable periods were evolved on the sample surface. As mentioned before, this paper is primarily focused on the HSFL, which is mostly developed at the edge of the irradiated spots. The evolution of these self-formed HSFLs printed on the titanium surface is represented by the SEM images of Fig. 2.

Self-formed HSFL are apparent on titanium surface after the application of 10 consecutive femtosecond laser pulses. HSFL are also observed after the illumination of 2000 laser pulses. The formation of HSFL beyond this limit is beyond the scope of this research. At low laser energy, HSFLs are evolved almost all over the irradiated area, especially, near the peripheral area of the irradiated spots as depicted in Fig. 2(a) to 2(f). With the increase of laser energy, ablative
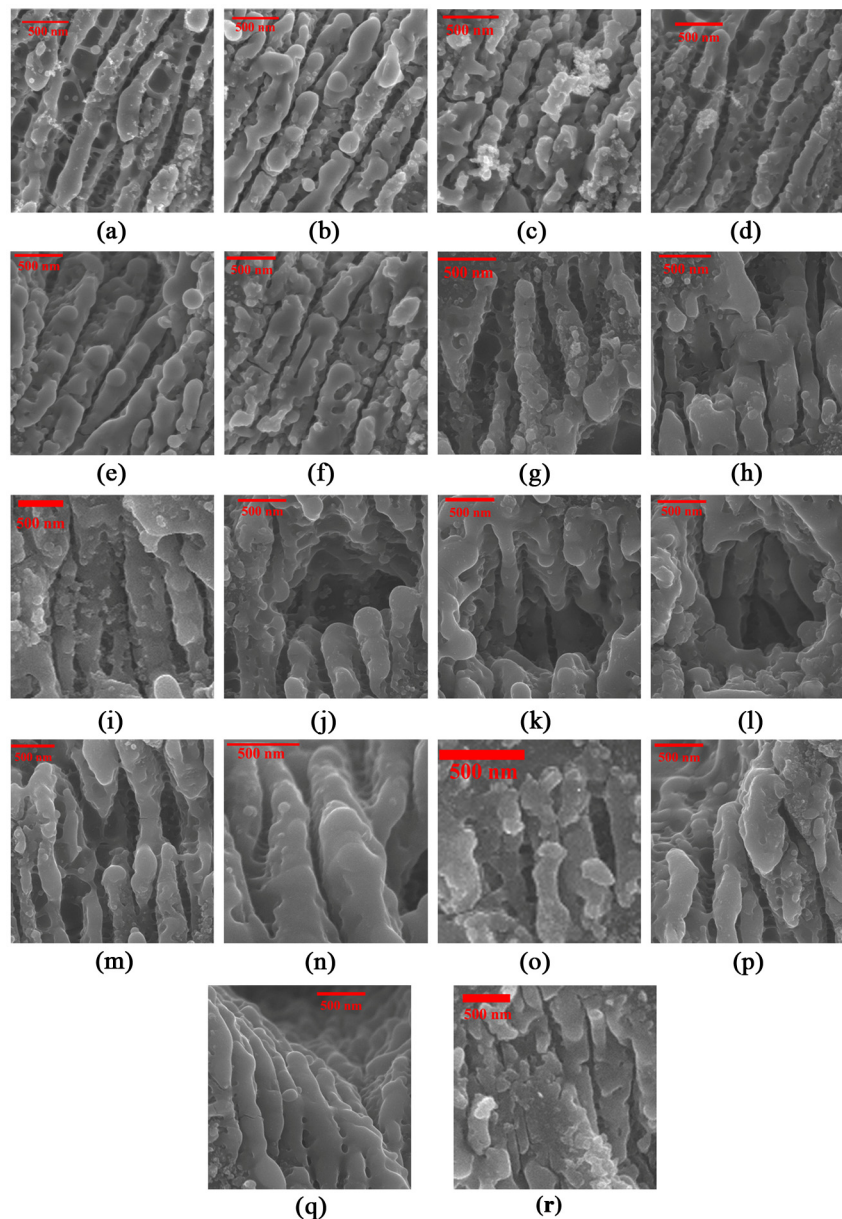

Fig. 2 SEM images of the self-organized nanogratings, fabricated on a titanium surface for various laser energy, pulse width, and number of laser pulses. (a)–(c) At laser energy (E_L) of 93 nJ, pulse width (τ) of 183 fs, and number of laser pulses (N) of 10, 500, 2,000; (d)–(f) $E_L = 93$nJ, $\tau = 500$ fs, and $N = 10, 500, 2,000$; (g–i) $E_L = 165$ nJ, $\tau = 183$ fs, and $N = 10, 500, 2,000$; (j–l) $E_L = 165$ nJ, $\tau = 500$ fs, and $N = 10, 500, 2,000$; (m–o) $E_L = 248$ nJ, $\tau = 183$ fs, and $N = 10, 500, 2000$; (p–r) $E_L = 248$ nJ, $\tau = 500$ fs, and $N = 10, 500, 2,000$.

craters start to form at the central part of each irradiated spot because of the Gaussian shape of the laser beam. As the laser energy increases, the size and the depth of the craters are increased. Beyond 165 nJ laser energy, ablative craters are expanded and severe damage is observed at the central part of the illuminated areas, which are evident from Fig. 2(g) to 2(r). As a result, the formation of HSFLs at the material surface is affected near the central part. However, HSFLs start to form at the bottom of the ablative craters. Although high laser energy affects the central part of the illuminated spots, HSFLs are always evident near the peripheral area of the ablated spots within the scope of our experimental conditions.

From the experimental results, we can infer that the orientation and the period of the HSFL have certain relationship to the irradiation conditions of the femtosecond laser beam. The direction of the self-formed HSFL is polarization dependent, irrespective of laser parameters. The HSFLs are perpendicular to the direction of the electric field vector of the femtosecond laser pulses. The periods of the HSFLs are influenced by laser energy, pulse width, and number of applied laser pulses. Figure 3 demonstrates the impact of average pulse energy, pulse width, and number of irradiated laser pulses on the fabrication of self-formed periodic HSFL and their period. The experimental results and their corresponding laser parameters for Fig. 3 are summarized in Table 1.

For a pulse width of 183 fs, the lowest period of the HSFL is 275 nm, which is observed at laser energy of 93 nJ after the irradiation of 2000 laser pulses. The lowest period of HSFL is 321 nm for a pulse width of 500 fs when laser energy is 93 nJ and the number of applied laser pulses is 2000. For a fixed pulse width and number of applied laser pulses, the period of the HSFL shows an increasing trend with the increase of average pulse energy of the femtosecond laser pulses. Unlike laser energy, the self-organized HSFLs are printed with lower periods, when the number of laser pulses increases by keeping the laser energy and the pulse width unchanged. Furthermore, when the laser energy and the number of irradiated laser pulses are constant, the nanograting period is influenced by the pulse width of the femtosecond laser pulses. The HSFL period increases with the increase of the pulse width, and vice versa.

4 Discussion

The self-formed nanogratings can be printed by applying several pulses at the same irradiated spot. As a result, long-period nanogratings are usually formed at the central part of the ablated area, known as LSFL, whereas short-period nanogratings are usually evident at the edge of the irradiated spot, known as HSFL, which is the primary focus of our investigation. At low laser energy, HSFL may evolve almost all over the irradiated area, as reported in Ref. 16. Until now, there is no defined threshold energy or formation region for LSFL and HSFL formations; however, there is clear evidence that the periods of the LSFL and the HSFL are quite different.[13,16]

Generally, the formation of LIPSS is characterized by the interaction of the ultrafast laser pulses with a metal surface.[13,14,20,21,24] According to Vorobyev et al.,[14] periodic LIPSS are printed on a metal surface due to the interference of excited surface plasmons with incident laser beam where the period of LIPSS follows a decreasing trend with the increase of laser pulses. However, the experimental results of the LIPSS period are quite different than their theoretical value ($d = \lambda/\eta$, where λ is the wavelength of the incident light and η is the refractive index of the material). One of the most significant results regarding LIPSS formation, reported in Ref. 14, is the correlation between the morphological clearness of LIPSS and the electron-phonon energy coupling coefficient (g); larger the value of g, much clearer the LIPSS pattern. This phenomenon, along with the electron diffusion effect on ripple growth, is further expanded by Colombier et al.[20] The researchers demonstrated that ripple amplitude is strongly influenced by the material transport properties, specifically electron-phonon relaxation strength, electronic diffusion, and the energy band characteristics of the electronic laser excitation. They showed the electronic temperature dependence of the electron diffusion depth,
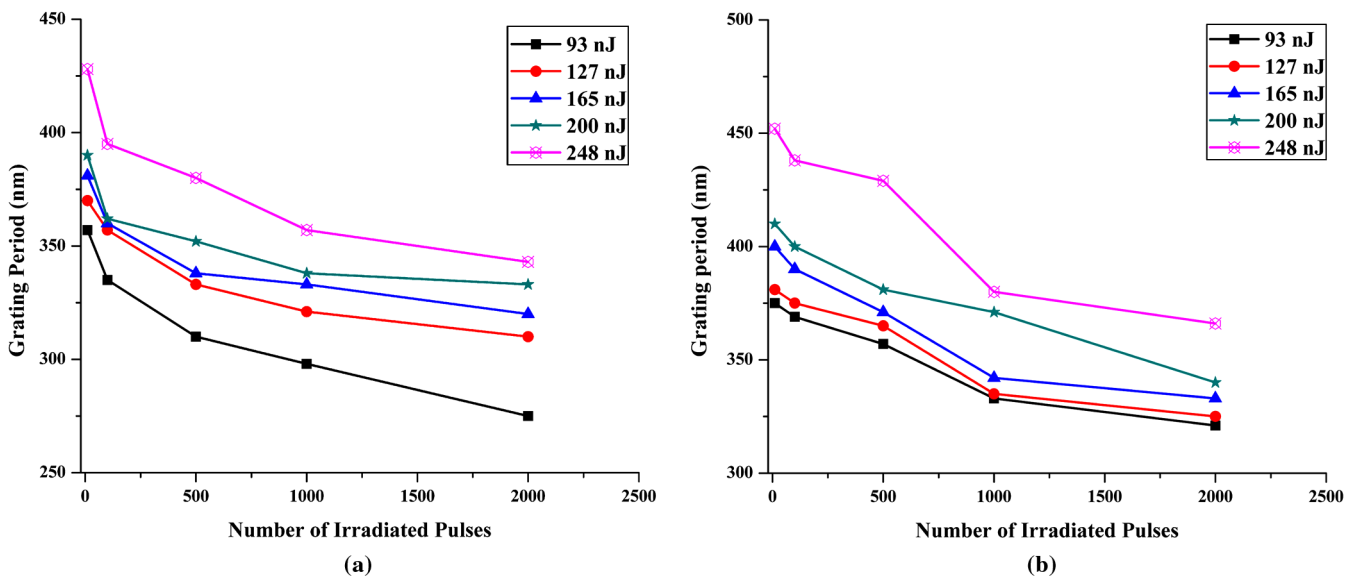

Fig. 3 Dependence of the periods of the nanogratings on the laser energy, the pulse width, and the number of irradiated laser pulses in each spot on a titanium surface. (a) For 183 fs laser pulses; (b) for 500 fs laser pulses.

Table 1 Summary of the experimental results and their corresponding laser parameters in Fig. 3.

Average period of the nanogratings at a pulse width of 183 fs					
	Laser energy (E_L)				
Number of laser pulses (N)	93 nJ	127 nJ	165 nJ	200 nJ	248 nJ
10	357 nm	370 nm	381 nm	390 nm	428 nm
100	335 nm	357 nm	360 nm	362 nm	395 nm
500	310 nm	333 nm	338 nm	352 nm	380 nm
1,000	298 nm	321 nm	333 nm	338 nm	357 nm
2,000	275 nm	310 nm	320 nm	333 nm	343 nm
Average period of the nanogratings at a pulse width of 500 fs					
	Laser energy (E_L)				
Number of laser pulses (N)	93 nJ	127 nJ	165 nJ	200 nJ	248 nJ
10	375 nm	381 nm	400 nm	410 nm	452 nm
100	369 nm	375 nm	390 nm	400 nm	438 nm
500	357 nm	365 nm	371 nm	381 nm	429 nm
1,000	333 nm	335 nm	342 nm	371 nm	380 nm
2,000	321 nm	325 nm	333 nm	340 nm	366 nm

which is different for different metals. Bonse et al.[13] have suggested that HSFLs are formed due to the nonlinear response of the surface structured with LSFLs, which can be considered as the involvement of a second-harmonic generation (SHG) at the rough surface. This model is further purified and elaborately explained by Golosov et al.[21] Due to the initial laser pulses, intermediate nonharmonic surface nanogratings (which can be considered as LSFLs) are printed on the metal surface, the spacing of which are equal to the first-harmonic period (Λ_1), which can be estimated by the SEW length Λ_{SEW} using the optical parameters of the excited metal.[21]

$$\Lambda_{SEW} = \lambda \left(\sqrt{\frac{Re\varepsilon_M Re\varepsilon_D}{Re\varepsilon_M + Re\varepsilon_D}} \pm \sin \theta_{inc} \right)^{-1}, \quad (1)$$

where ε_M and ε_D are the permittivity of the metal and dielectric at the wavelength λ, and θ_{inc} is the angle of incidence. When more laser pulses are applied, they are diffracted from the intermediate nonharmonic periodic nanogratings and 1-D periodic nanogratings (which can be considered as HSFLs), and the harmonics of the nanorelief are produced with spacing $\Lambda_m = \Lambda_1/m \ll \Lambda_1$ (m is the harmonic order).[21] From the aggregation of all the previous analysis, we can infer the formation mechanism of the self-organized LIPSS (HSFL, in our case) on our titanium sample, which can be interpreted by the following explanation.

LIPSS formation is a natural phenomenon of solids that are originated from the interference of the incident and reflected/refracted laser pulses with the scattered (diffracted) light near the metal-dielectric interface. Diffraction of incident laser pulses is caused due to the micro- or nano-metric roughness of the surface, defects, and spatial variations in the dielectric constant.[24] For an optically active material like titanium, when femtosecond laser pulses are applied, plasmon-polariton waves (i.e., SEWs) are excited on the metal surface, which undergoes interference with the incident laser pulses and, as a consequence, intermediate nanogratings (LSFLs) with fundamental harmonic period (Λ_1) is evolved on the metal surface; Λ_1 can be approximated by Eq. (1). When more laser pulses are applied at the same spot, LIPSS are reprinted again and again at the same point of the metal surface with the periods of varying gratings, which are evolved due to the diffraction of incident laser pulses from the intermediate surface gratings. The depth and width of the nanogratings depend on the electron-phonon coupling strength and the electron diffusion.[20]

We also examine the intensity profile and amplitude spectra of fast Fourier transform (FFT) for the surface nanogratings (in this case, HSFLs) produced on the titanium surface during our experiment, which is represented in Fig. 4. We scanned in the direction perpendicular to the nanograting orientation of Fig. 2(a), 2(f), 2(k), and 2(p) to obtain intensity profile-related information as depicted in Fig. 4(a) to 4(d). Amplitude spectra of FFT for Fig. 2(a), 2(f), 2(h), and 2(p)
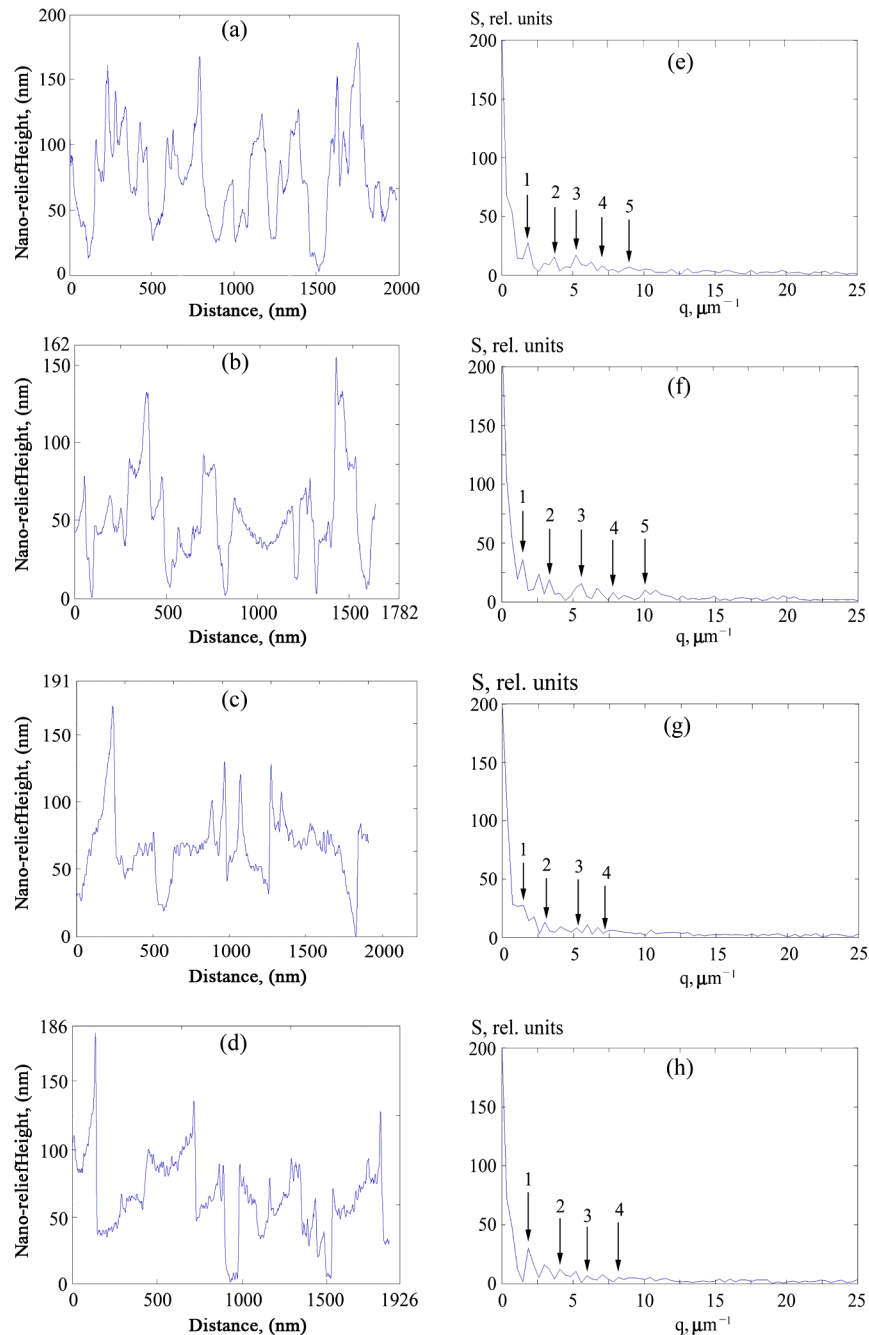
Fig. 4 (a)–(d) Nano-relief height for Fig. 2(a), 2(f), 2(k), and 2(p). (e)–(h) Amplitude spectra of the FFT for the surface nanogratings presented in Fig. 2(a), 2(f), 2(k), and 2(p); the arrows with numbers show the position of the corresponding harmonics of the nanogratings.

are represented in Fig. 4(e) to 4(h). From the amplitude spectra of Fig. 4(e) to 4(h), it is obvious that the HSFLs are originated due to the generation of higher-order harmonics on the titanium surface because of diffraction of incident laser beam from the initially formed nonlinear surface gratings.

With the increase of laser pulses, the harmonic order is expected to be increased. As a result, the periods of the reprinted LIPSS are expected to show a decreasing trend with the increase of the number of laser pulses; and consequently, HSFLs are formed with a lower grating period, which is in reasonable agreement with our experimental results.

The intensity of the diffracted waves depends on the irradiation conditions of the laser pulses and the material type. The diffraction efficiency, which is determined by the ratio of the power of the diffracted light (P_{diff}) to the incident power of the laser beam (P_{inc}), is a function of refractive index change (Δ_η). The mth order diffraction efficiency (n_m) can be written as follows:[25]

$$n_m = [J_m(2\pi d\Delta\eta/\lambda \cos \theta)]^2, \tag{2}$$

where $J_m(\delta)$ is a Bessel function, d is the thickness of the grating, Δ_η is the refractive index change, λ is the wavelength of the incident beam, and θ is the incident angle.

The change in laser energy might have altered the periodic modulation of the absorbed light intensity caused by the variation of interference patterns of the incident laser beam and the surface plasmon-polariton waves (SEWs); consequently, the fundamental harmonic period Λ_1 is altered. This phenomena might have influenced the period of the surface nanorelief of higher-order harmonics Λ_m (period of HSFL), which have shown an increasing trend with the increase of laser energy.

Like laser energy, due to the change of pulse duration, the surface electron density and the electron density of the plasma are expected to be altered. The refractive index of the titanium surface is expected to change as well, which in turn influences the diffraction efficiency and the interference pattern of the SEWs and the incident laser beam. Aggregation of all these effects might have caused the increase of the periods of the nanogratings with the increase in width of the femtosecond laser pulses.

With the increase of laser energy, ablative craters are evident near the central part of the ablated area. Since the ablated craters' walls are curved, the polarization state of the laser pulses and their incident angles are expected to be different for different positions of the wall.[15] These phenomena may significantly influence the LIPSS period formed inside the craters. However, the primary focus of this article is HSFLs, which are mainly formed near the peripheral part of the irradiated spot. Thus, we can expect that the polarization state and their incident angle have negligible influence on the HSFL period.

5 Conclusion

In summary, we investigated the evolution of self-organized nanogratings, especially HSFLs, on a titanium surface. We noticed the polarization dependence of the orientation of the nanogratings, which were formed in the perpendicular direction of the electric field vector. We noticed the dependence of the HSFL period on various laser parameters, including the average pulse energy, pulse width, and number of irradiated laser pulses. We discovered the tendency of the HSFL period to increase with the increase of laser energy and pulse width of the femtosecond laser pulses. At the same time, HSFL periods have shown a trend to decrease with the increase of irradiated laser pulses. In addition, we explained the formation mechanism of the self-formed nanogratings (LSFLs and HSFLs) and the reason behind the variation of HSFL periods with the irradiation conditions of the femtosecond laser pulses. We strongly believe that our experimental results will assist to understand the interactions of the femtosecond laser pulses with titanium and the mechanism behind the formation of self-organized nanogratings on a titanium surface.

References

1. T. H. Maiman, "Stimulated optical radiation in ruby," *Nature* **187**(4736), 493–494 (1960).
2. L. Qi, "Microstructures fabrication using femtosecond laser," Ph.D. thesis, (Chubu University, Aichi, Japan, 2010).
3. B. Wu et al., "Superhydrophobic surfaces fabricated by microstructuring of stainless steel using femtosecond laser," *Appl. Surf. Sci.* **256**(1), 61–66 (2009).
4. B. K. Nayak, M. C. Gupta, and K. W. Kolasinski, "Formation of nano-textured conical microstructures in titanium metal surface by femtosecond laser irradiation," *Appl. Phys. A* **90**(3), 399–402 (2008).
5. M. S. Ahsan, Y. G. Kim, and M. S. Lee, "Formation mechanism of nanostructures on the stainless steel surface by femtosecond laser pulses," *J. Laser Micro/Nanoeng.* **7**(2), 164–170 (2012).
6. M. Alubaidy, K. Venkatakrishnan, and B. Tan, "Fabrication of a reinforced polymer microstructure using femtosecond laser material processing," *J. Micromech. Microeng.* **20**(5), 055012 (2010)
7. M. S. Ahsan et al., "Colorizing stainless steel surface by femtosecond laser induced micro/nano-structures," *Appl. Surf. Sci.* **257**(17), 7771–7777 (2011).
8. G. A. Torchia et al., "Laser gain in femtosecond microstructured $Nd:MgO:LiNbO_3$ crystals," *Appl. Phys. B* **83**(4), 559–563 (2006).
9. M. S. Ahsan, Y. G. Kim, and M. S. Lee, "Formation mechanism of nanostructures in soda-lime glass using femtosecond laser," *J. Non-Cryst. Solids* **357**(3), 851–857 (2011).
10. Y. Shimotsuma et al., "Self-organized nanogratings in glass irradiated by ultrashort light pulses," *Phys. Rev. Lett.* **91**(24), 247405 (2003).
11. V. R. Bhardwaj et al., "Optically produced arrays of plannar nanostructures inside fused silica," *Phys. Rev. Lett.* **96**(5), 057404 (2006).
12. C. W. Cheng et al., "Fabrication of micro/nano crystalline ITO structures by femtosecond laser pulses," *Appl. Phys. A* **101**(2), 243–248 (2010).
13. J. Bonse, M. Munz, and H. Sturm, "Structure formation on the surface of indium phosphide irradiated by femtosecond laser pulses," *J. Appl. Phys* **97**(1), 013538 (2005).
14. A. Y. Vorobyev, V. S. Makin, and C. Guo, "Periodic ordering of random surface nanostructures induced by femtosecond laser pulses on metals," *J. Appl. Phys.* **101**(3), 034903 (2007).
15. Y. Huang et al., "Two-dimensional periodic structure induced by single-beam femtosecond laser pulses irradiating titanium," *Opt. Exp.* **17**(23), 20756–20761 (2009).
16. L. Qi, K. Nishii, and Y. Namba, "Regular subwavelength surface structures induced by femtosecond laser pulses on stainless steel," *Opt. Lett.* **34**(12), 1846–1848 (2009).
17. S. Sakabe et al., "Mechanism for self-formation of periodic grating structures on a metal surface by a femtosecond laser pulse," *Phys. Rev. B* **79**(3), 033409 (2009).
18. K. Okamuro et al., "Laser fluence dependence of periodic grating structures formed on metal surfaces under femtosecond laser pulse irradiation," *Phys. Rev. B* **82**(16), 165417 (2010).
19. E. V. Golosov et al., "Femtosecond laser writing of subwave one-dimensional quasiperiodic nanostructures on a titanium surface," *JETP Lett.* **90**(2), 107–110 (2009).
20. J. P. Colombier et al., "Effects of electron-phonon coupling and electron diffusion on ripples growth on ultrafast-laser-irradiated metals," *J. Appl. Phys.* **111**(2), 024902 (2012).
21. E. V. Golosov et al., "Ultrafast changes in the optical properties of a titanium surface and femtosecond laser writing of one-dimensional quasi-periodic nanogratings of its relief," *JETP* **113**(1), 14–26 (2011).
22. A. M. Bonch-Bruevich et al., "Surface electromagnetic waves in optics," *Opt. Eng.* **31**(4), 718–730 (1992).
23. M. S. Ahsan, "Formation of micro/nano-structures on glasses and metals using femtosecond laser and their applications," Ph.D. thesis, Korea Advanced Institute of Science and Technology (KAIST), Daejeon, South Korea (2012).
24. D. Bäuerle, *Laser Processing and Chemistry*, Springer, New York (2000).
25. Q. Z. Zhao et al., "Temperature dependence of femtosecond laser induced refractive index change Nd3+-doped phosphate glass," *Opt. Mater.* **27**(6), 1159–1162 (2005).

Md. Shamim Ahsan received his integrated MS/PhD degree in information and communications engineering from the Korea Advanced Institute of Science and Technology (KAIST), Daejeon, South Korea, in 2012. He received his BSc Engg degree in electronics and communication engineering from Khulna University, Khulna, Bangladesh. He served as a lecturer in Khulna University, Khulna, Bangladesh, from December 2003 to February 2007. He has been serving as an assistant professor at the same university since February 2007. He is currently working as a postdoctoral researcher at the Information and Electronics Research Institute, KAIST, Daejeon, South Korea, since February 2012.

Man Seop Lee received his BSc and MSc degrees from Busan National University, South Korea, in 1976 and 1978, and PhD degree from Korea Advanced Institute of Science and Technology (KAIST), South Korea, in 1991, all in Electrical Engineering. He was a director of Electronics and Tele-communications Research Institute (ETRI), South Korea during 1979 to 1997. He served as an adjunct professor at the Chun-Buk University, South Korea during 1993 to 1997. He was employed as a professor in the Information and Communications University (ICU), South Korea from 1998 to 2009. He served as the director of the ICU Joint Research Center and ICU Venture from 1998 to 2005. He was the Dean of the ICU, Office of Planning Affairs from 2008 to 2009. Since 2009, he has been serving as a professor at KAIST, South Korea. His research interests are currently focused on femtosecond laser based micro/nano-machining of various materials.